Automatic Reactive Power Compensation utilizing Variable Excitation Capacitance for Wind Turbine Employing SEIG for Feeding IM Driving Centrifugal Pump

Mohammed I. Abuashour[1a], Tha'er O. Sweidan[2b], Audai Al-Kurdi[1c], Mohammed Al-maaitah[1d]
Waleed Hammad[3e], Mohammed alhattab[1f], Omar Abdallah[3g]

[1] *Electrical Engineering Department, The Hashemite University, Zarqa 13115, Jordan*
[2]*Electrical Engineering Department, Higher Colleges of Technology, Sharjah Colleges,7947 Sharjah, UAE*
[3]*Mechanical Engineering Department, The Hashemite University, Zarqa 13115, Jordan*

Abstract — *This paper presents a stand-alone wind power system supplying a three- phase induction motor for pumping applications. The nonlinear dynamical mathematical model for the system components is presented and used for the numerical simulations. The system comprises a wind turbine driving a self-excited induction generator (SEIG) terminated by capacitor bank. This energy source feeds (IM) driving a centrifugal pump. The voltage regulation is established through a voltage controller by changing the excitation capacitance that provides the reactive power needed for self-excited induction generator in response to any voltage fluctuations that might occur during the system normal operation or the load variations. The system performance is tested by changing the load torque coupled to the motor. It is shown that the system has an excellent ability to run smoothly at a wide range of motor loading conditions by changing the excitation levels as a result of changing capacitor bank which indicates the robustness and proves the reliability of the integration between different system components. Numerical simulations are executed using MATLAB software.*

Keywords — *Self-excited induction generator; SEIG; Wind system; Induction motor; IM; Dynamical analysis; voltage controller.*

I. INTRODUCTION

As the world population is increasing in alarming rates [1], the demand for renewable energy resources became one of the world's crucial concerns. So many researches are conducted recently in this field. Furthermore, the environment concerns and other related issues have triggered the attention for the use of renewable energy resources for example wind, solar, fuel cells, water power etc., as solutions for the anticipated serious problem in many countries. The signs of the global energy crisis motivate scientists and researchers from all over the world to increase their interest in the SEIG for huge potentials for renewable energy resource. The SEIGs are increasingly considered for remote applications. SEIG are appropriate for rural areas applications because of their economic cost, operational simplicity, low maintenance burden, and no extra excitation supply are the chief benefits of utilizing the SEIG for power generation [2].The stand-alone self-excited induction generator is primarily IM that is driven by a prime mover, while using an external capacitor bank connected to its stator terminals for building the air-gap flux, and supplying reactive power to the load. The SEIG loads might be static and dynamic loads. Lots of research concentrated upon the static loads coupled to SEIG [3].The research on dynamic IM load is limited to steady-state analysis. For instance, an effort to study the behavior of the SEIG with the IM load is firstly presented in [4] and later is presented in [5]. The transient analysis of the stand-alone SEIG with the IM load is lately addressed in [6], [7]. This refers to study scarcity in this aspect so the transient and steady state performance of the SEIG and IM load have to be further investigated even with voltage regulators and variable loading. In this paper, dynamical and steady state simulations of a wind turbine using SEIG feeding IM load for pumping application is investigated with voltage controller using variable capacitance to supply the needed reactive power. Transient and steady state performance are presented when a load coupled to IM shaft is changed and the capacitance value is automatically changed in accordance with any voltage variation to supply the reactive power for SEIG and keeping the IM terminal voltage constant. The implementation of the system components dynamical nonlinear models are presented in MATLAB environment. Perturbation and Observation examined as MPPT excellent technique for PV generator electrically integrated to

the grid is examined by carrying out Large-signal stability analysis through three-phase to ground symmetrical fault imposed in the middle length of one phase from transmission power phases as the PV system is exposed to different insolation levels, the related simulated numerical results reveals that the highly PV penetrated grid sustains stability and also determined that the overshoot and the settling time are extremely influenced by the fault clearing time and insolation, as the insolation level gets higher, the critical clearing time and the overshoot get higher and the settling gets lower accordingly [8]. The model demonstrating the transient and the steady state conditions for permanent magnet, shunt and series motors powered by PV system is presented and tested for different insolation levels. The outcomes are compared to results obtained by using fixed voltage source for powering the motors which reveals a good matching and a wide range of stable operating points [9]. FOCV technique as MPPT scheme for the dynamical and transient study of DC series motor and AC three phase induction motor supplied by a PV system at different insolation levels and various motor loading is examined [10]. The transient behavior of a shunt Grouping of DC Shunt Motor and an induction motor supplied by standalone PV power plant at different insolation levels is inspected, the MPPT for the PV system was achieved for different insolation levels, the intended study investigated firstly the system reaction at different insolation levels and changing the loading torque for both motors and secondly subsequent step alteration in insolation levels with unchanging loading torques for both motors [11]. a DC shunt motor electrically powered and excited by PV system for feeding the armature and the field circuits. FOCV method is employed for tracking the MPP by synchronously varying the duty cycle of the DC-DC buck-boost power converter and thus keeping the terminal voltage of DC-DC converters equals to the instantaneous one at the maximum power point drawn from the PV power system [12]. Perturbation and Observation technique as maximum power point tracking method for the dynamical analysis of DC shunt motor and DC series motor fed by a photovoltaic generator at different solar irradiance levels and various motor loading conditions is investigated [13,14].

In this paper a stand-alone wind power system supplying a three- phase induction motor for pumping applications is proposed. The nonlinear dynamical mathematical model for the proposed system components is presented and used for the numerical simulations. The system comprises a wind turbine driving a self-excited induction generator (SEIG) terminated by capacitor bank. The induction motor driving a centrifugal pump is supplied by the wind turbine. The voltage regulation strategy is made through a voltage controller the common coupling point by varying the excitation capacitance that furnishes the reactive power needed for self-excited induction generator in response to any voltage fluctuations that might occur during the system normal operation or the load variations. The system performance is tested after a successive step changes in the load torque coupled to the motor which indicate reliability of the integration between different parts of the system under study .This paper is structured in the following manner: Section 2 describes the configuration of the system under study. The dynamical mathematical model of all power system components are outlined in Section 3. The numerical simulations and discussions are addressed in Section 4 and finally conclusions are presented in Section 5.

II. SYSTEM CONFIGURATION AND DESCRIPTION

Figure 1 shows the schematic diagram for the stand-alone power system. It is an energy system which comprises a wind-driven self-excited squirrel-cage induction generator at the coupling point the mandatory lumped capacitance for the three-phase induction generator connected to its stator which is used to provide the induction generator with its reactive power requirements. This energy system is used to feed a three-phase squirrel-cage induction motor that is driving mechanically a coupled pump to its shaft.

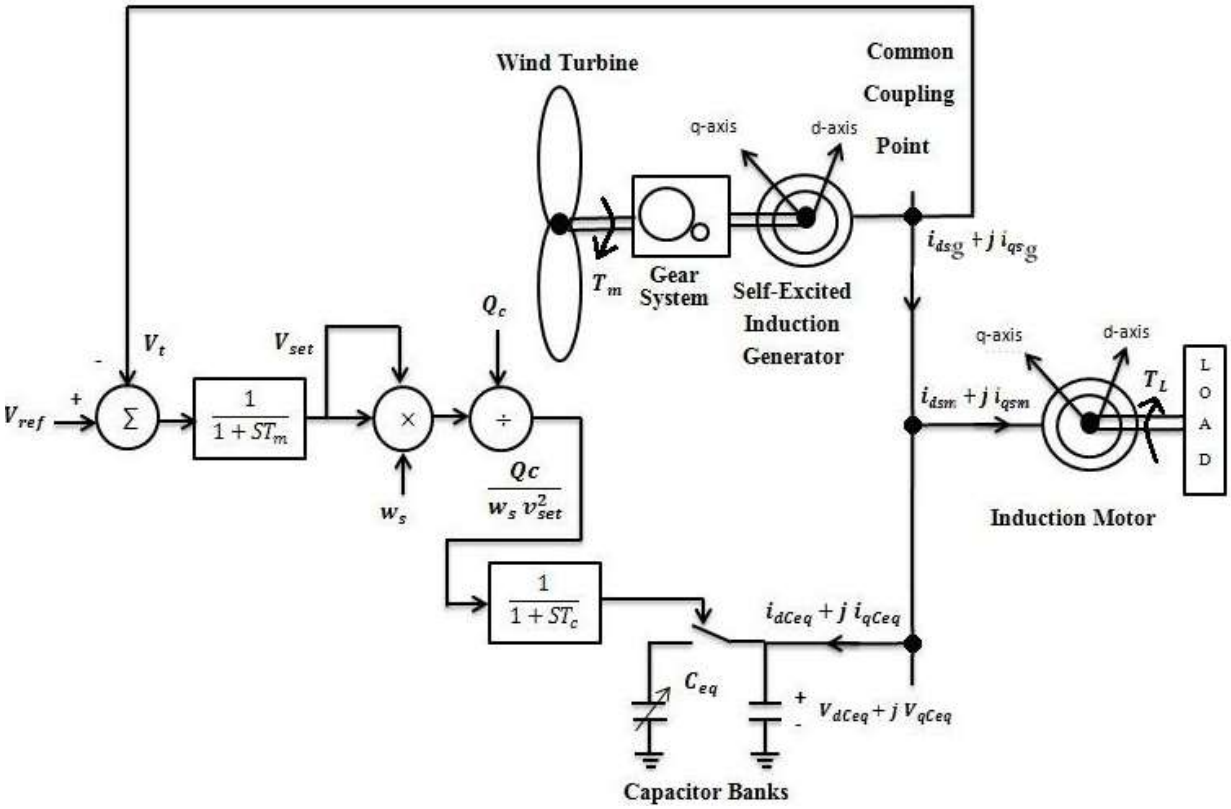

Figure 1. Schematic diagram for the power system under study

III. WIND TURBINE GENERATOR DESIGN AND THE SYSTEM DYNAMICAL MODEL

This section presents the mathematical equations representing the dynamics of the system and is also summarized for all system components in their nonlinear form as projected on the synchronously rotating d-q reference frame.

A. Three-phase induction motor

The nonlinear dynamical mathematical model of squirrel cage Three-phase induction motor in synchronously rotating d-q reference frame can be summarized as [15]:

$$L_{ssm}\frac{di_{sdm}}{dt} + L_{mm}\frac{di_{rdm}}{dt} = V_{ds} + \omega_s L_{ssm} i_{sqm} + \omega_s L_{mm} i_{rqm} - R_{sm} i_{sdm} \quad (1)$$

$$L_{ssm}\frac{di_{sqm}}{dt} + L_{mm}\frac{di_{rqm}}{dt} = V_{qs} - \omega_s L_{ssm} i_{sdm} - \omega_s L_{mm} i_{rdm} - R_{sm} i_{sqm} \quad (2)$$

$$L_{mm}\frac{di_{sdm}}{dt} + L_{rrm}\frac{di_{rdm}}{dt} = V_{dr} + (\omega_s - \omega_{rm}) L_{rrm} i_{rqm} + (\omega_s - \omega_{rm}) L_{mm} i_{sqm} - R_{rm} i_{rdm} \quad (3)$$

$$L_{mm}\frac{di_{sqm}}{dt} + L_{rrm}\frac{di_{rqm}}{dt} = V_{qr} - (\omega_s - \omega_{rm}) L_{rrm} i_{rdm} - (\omega_s - \omega_{rm}) L_{mm} i_{sdm} - R_{rm} i_{rqm} \quad (4)$$

$$J_m\frac{d\omega_{rm}}{dt} = \frac{3P_m}{4}\left(L_{mm} i_{rdm} i_{sqm} - L_{mm} i_{rqm} i_{sdm}\right) - T_{Lm} \quad (5)$$

B. Three-phase induction generator and wind turbine)

The nonlinear dynamical mathematical model of squirrel cage three-phase induction generator in synchronously rotating d-q reference frame can be summarized as [15]:

$$L_{ssg}\frac{di_{sdg}}{dt} + L_{mg}\frac{di_{rdg}}{dt} = -V_{ds} + \omega_s L_{ssg} i_{sqg} + \omega_s L_{mg} i_{rqg} - R_{sg} i_{sdg} \quad (6)$$

$$L_{ssg}\frac{di_{sqg}}{dt} + L_m\frac{di_{rqg}}{dt} = -V_{qs} - \omega_s L_{ssg} i_{sd} - \omega_s L_{mg} i_{rdg} - R_{sg} i_{sqg} \quad (7)$$

$$L_{mg}\frac{di_{sdg}}{dt} + L_{rrg}\frac{di_{rdg}}{dt} = V_{dr} + (\omega_s - \omega_{rg})L_{rrg} i_{rqg} + (\omega_s - \omega_{rg})L_{mg} i_{sqg} - R_{rg} i_{rdg} - Kd \quad (8)$$

$$L_{mg}\frac{di_{sqg}}{dt} + L_{rrg}\frac{di_{rqg}}{dt} = V_{qr} - (\omega_s - \omega_{rg})L_{rrg} i_{rdg} - (\omega_s - \omega_{rg})L_{mg} i_{sdg} - R_{rg} i_{rqg} - Kq \quad (9)$$

$$J_g\frac{d\omega_{rg}}{dt} = T_{Lg} - \frac{3Pg}{4}(L_{mg} i_{rqg} i_{sdg} - L_{mg} i_{rdg} i_{sqg}) \quad (10)$$

The magnetization characteristic of the SEIG is nonlinear. The relationship between magnetizing inductance L_m and magnetizing current i_m is obtained from synchronous speed tests. A fifth degree polynomial is used for representing the magnetizing inductances against magnetizing current [16, 17]. This is given by the following polynomial:

$$Lm = a_5 im^5 + a_4 im^4 + a_3 im^3 + a_2 im^2 + a_1 im + a_0 \quad (11)$$

Wherea_5,a_4,a_3,a_2,a_1, and a_0 are constants obtained via curve fitting for the characteristic curve of Figure 2. The values of these constants are given in the Appendix B [17].

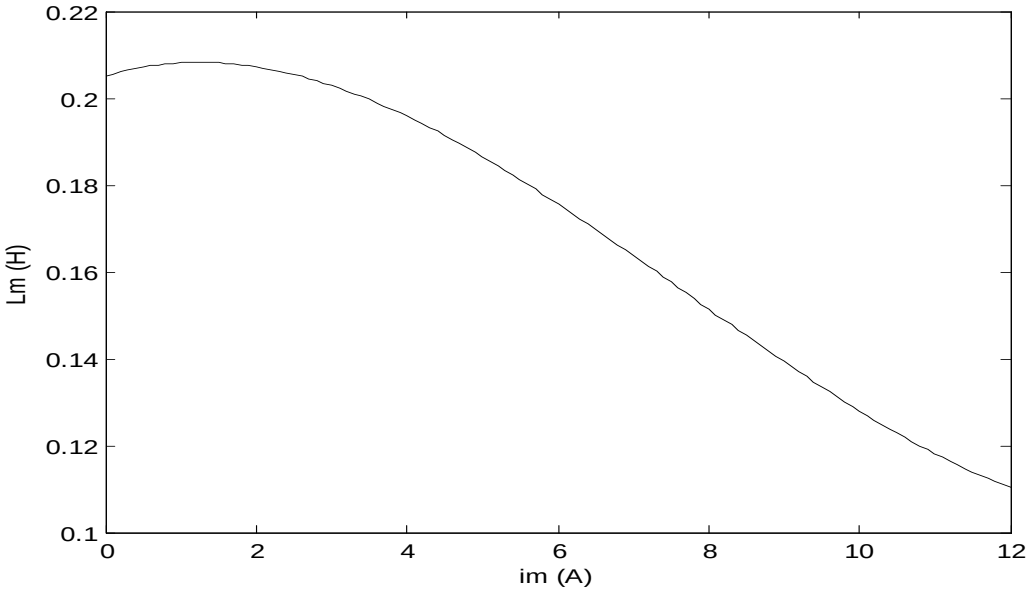

Figure 2. Magnetizing inductances against the magnetizing current

The variable T_{Lg}appearing in equation (10) is the deriving torque of the induction generator developed by the wind turbine as shown in Figure 1. Wind turbine is a mechanical device which converts the kinetic energy associated in air into mechanical power. The rotating motion of the turbine blades coupled to the gear box forces the shaft of the electric generator to rotate higher than the synchronous speed. Power captured by wind turbine blade is related to the blade shape, the pitch angle, speed of rotation and the radius of the rotor [18].
The power developed by a wind turbine is :

$$P_T = \frac{1}{2}\pi\rho C_p(\lambda,\beta)R^2V^3 \quad (12)$$

Where ρ is the air density (kg/m3),$C_P$is the power coefficient with a maximum value equal to 0.48 at particular wind speed, *R* is the radius of the wind blades (m) and *V* is the speed of wind (m/s). It normally employs an induction generator. Capacitor bank is necessary to supply the induction generator with reactive power. Rotor blades pitch angle control is one possible technique widely used to regulate the speed of the turbine [19]. The rated rotational speed of electrical generators is normally much higher than that of wind turbines and therefore a speed step-up gear system is employed as intermediate stage between the turbine and the generator as shown in Figure 1.

C. Design of Excitation Capacitance for Self-Excited Induction Generator

The excitation capacitance value was determined in reference to [20] this method based on the steady state equivalent circuit for computing the minimum value of capacitance to initiate self-excitation in the SEIG for maintaining the terminal voltage constant when the SEIG is loaded.

D. Centrifugal Pump Model

Centrifugal pump is used for low head applications. This pump is has rotary impeller. It throws the water radially so that the water momentum is transformed into useful pressure for lifting. The centrifugal pump has high efficiency, with lower speeds. The pump is assisted by its mechanical power on its shaft coupled to the pump, which is given by [21].

$$P_m = \frac{\rho g R D}{\eta} \quad \text{Watts} \tag{13}$$

The useful power is given by,

$$P_u = \rho g R D \quad \text{Watts} \tag{14}$$

ρ: Density of water (Kg/m3),g: Gravitational acceleration (m/sec^2), R: Total head height (m), D: Discharge flow rate (m^3/sec), η: Efficiency of pump.

E. Voltage Controller Model

The voltage of coupling bus is measured as follows [22]

$$V_t = \sqrt{V_{cd}{}^2 + V_{cq}{}^2} \tag{15}$$

This voltage is compared with some reference V_{ref}value the resulting component is V_{set}

$$T_M \frac{dV_{set}}{dt} = (V_{ref} - V_t) - V_{set} \tag{16}$$

Then the Capacitor reactive power is measured by

$$Q_C = (V_{qc}{}^2 * I_{dc}{}^2 - V_{dc}{}^2 * I_{qc}{}^2) \tag{17}$$

The capacitance value is found by the following equation

$$T_D \frac{dC}{dt} = \frac{Q_C}{w_s * V_{set}{}^2} - C \tag{18}$$

IV. Numerical Simulations and Discussions for the System Response at Different Induction Motor Loading Conditions

This section presents the numerical simulations of the nonlinear dynamical model of the system after step changes in the mechanical load coupled to the motor. Figures 3 presents the response of the system as the load torque (*TL*) has step change from 22.5 Nm to 17.5 Nm to 12.5 Nm. The induction motor operating points as follows: At 22.5 Nm the phase voltage is 127V, the capacitance value is 1.903mF the IM current is 11.3A the IG current is 15.5A the excitation capacitance current is 4.323A. At 17.5 Nm the phase voltage is 127V, the capacitance value is 1.819mF the IM current is 10.36A the IG current is 14.92A the excitation capacitance current is 4.307A. At 12.5 Nm the phase voltage is 127V, the capacitance value is 1.708mF the IM current is 10.45A the IG current is 14.45A the excitation capacitance current is 4.282A.

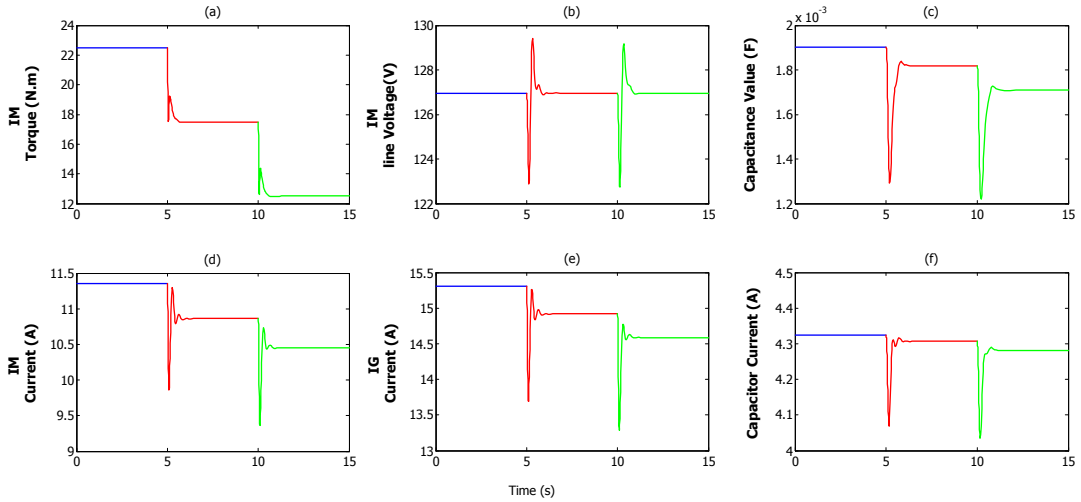

Fig.3.(a) Induction motor induced torque, (b) IM Phase voltage, (c) Capacitance Value (d) IM current (e) IG current (f) Capacitor current after step change of the load coupled to the motor from 22.5 nm to 17.5 nm to 12.5 nm

Figures 4 also presents the response of the system as the load torque (*TL*) has step changed from 22.5 Nm to 17.5 Nm to 12.5 Nm. During these numerical simulations, it is found that at 22.5 Nm the IG active power is 6.15KW, the IM active power is6.15KW,the IG reactive power is 4.958KVAr, the IM reactive power is 4.109KVAr, the excitation capacitance reactive power is 11.48 KVAr and the IM rotational speed is 1783rpm. In the same fashion at 17.5.5 Nm the IG active power is 4.869KW, the IM active power is 4.869KW, the IG reactive power is 4.92KVAr, the IM reactive power is 4.083KVAr, the excitation capacitance reactive power is 11.41 KVAr, and the IM rotational speed is 1786rpm. Similarly at 12.5 Nm the IG active power is 3.592KW, the IM active power is 3.592KW, the IG reactive power is 4.862KVAr, the IM reactive power is 4.043KVAr, the excitation capacitance reactive power is 11.31 KVAr, and the IM rotational speed is 1790rpm.

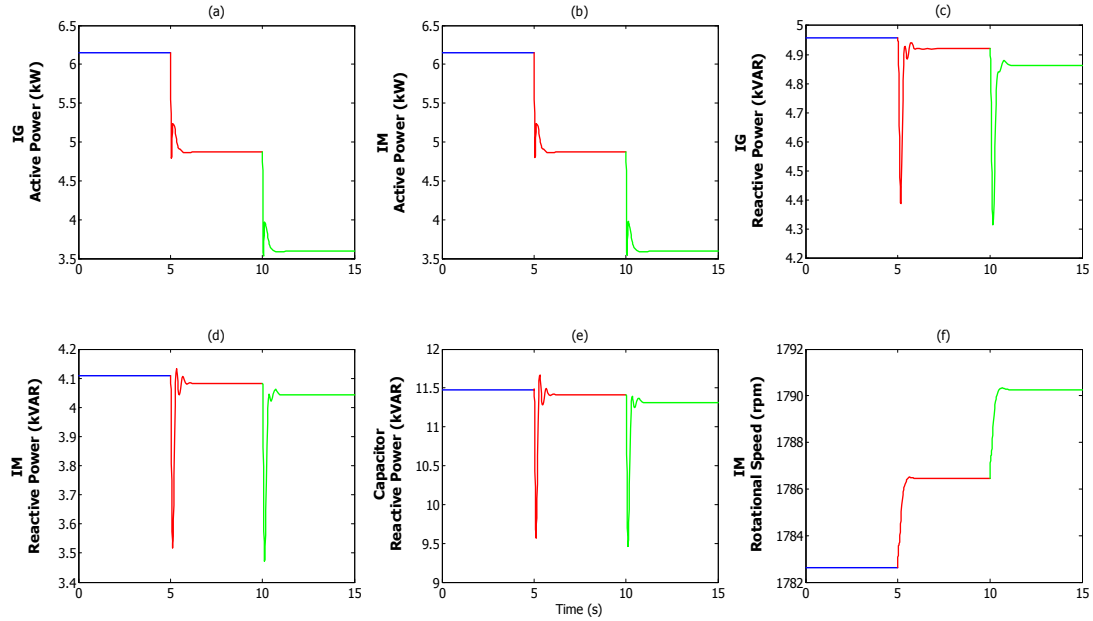

Fig.4. (a) IG active power (b) IM active power (c) IG reactive power (d) IM reactive power (e) Capacitor reactive power (f) IM rotational speed after step change of the load coupled to the motor from 22.5 nm to 17.5 nm to 12.5nm.

For the steady-state output characteristics the operating points of the systems are obtained by dropping out all the time derivative terms of the dynamical differential equations that describe the whole system and solving the resulting nonlinear algebraic equations using the MATLAB software.Figure5shows the steady-state output characteristics (torque-speed characteristics) for the induction motor which complies strongly as it is compared with the well-known characteristics of the electrical machines operation in general (The higher the load torque the lower the speed).

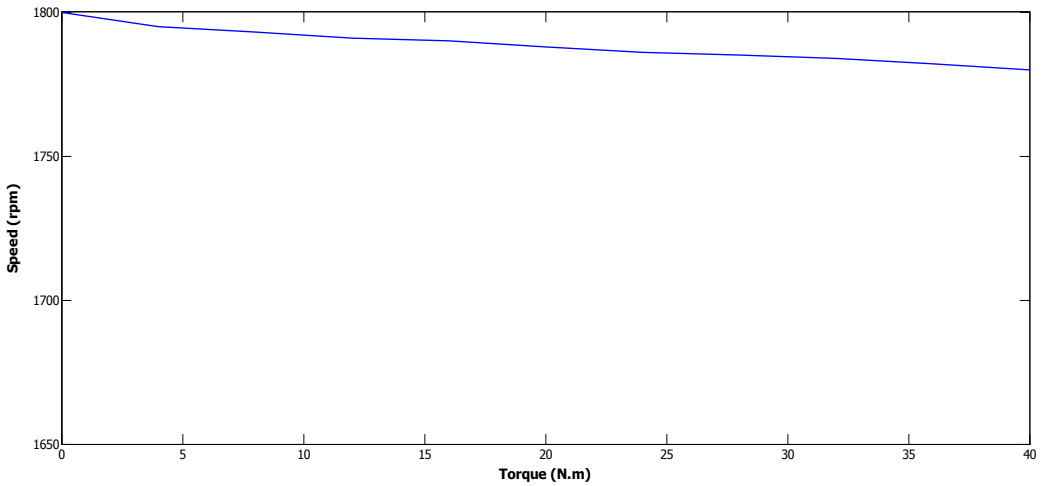

Fig. 5. The torque speed characteristics of Induction motor

As a summery for the steady-state system parameters for all running conditions, Table I shows the values for the stand-alone power system after step change of the load coupled to the motor from 22.5 nm to 17.5 nm to 12.5 nm.

Table 1. Steady-state parameters of the power system at three different motor loading conditions

Different Electrical Quantities	**Loading Conditions (N.m)**		
	22.5	**17.5**	**12.5**
Induction motor current (A)	11.36	10.36	10.45
Induction generator current (A)	15.3	14.92	14.59
Capacitor current (A)	4.323	4.307	4.282
Induction motor active power (kW)	6.15	4.869	3.592
Induction generator active power (kW)	6.15	4.869	3.592
Induction generator reactive power (kVAr)	4.958	4.92	4.862
Induction motor reactive power (kVAr)	4.109	4.083	4.043
Capacitor reactive power(kVAr)	11.48	11.41	11.31
Phase voltage (V)	127	127	127
Induction motor speed (rpm)	1783	1786	1790

Capacitance Value(mf)	1.903	1.819	1.708
Mechanical power (kW)	4.198	3.271	2.342

V. CONCLUSIONS

The automatic reactive power compensation for the Wind Turbine employing SEIG for feeding IM for Driving a Pump utilizing a Variable Excitation Capacitance is investigated. The Energy system comprises a wind turbine driving a self-excited squirrel-cage induction generator feeds a three-phase squirrel-cage induction motor for driving centrifugal pump. The main purpose of implementing the capacitance with the stator of the induction generator is to feed it with its reactive power need. The study comprises the response of the power system after step change in the load coupled to the motor. It is concluded that the proposed power system can run steadily at wide range of the motor loading conditions. It is found that the power consumed by the motor is equal to the power generated by SEIG generator. Basically, as the mechanical load coupled to the motor increases, the rotational speed of the motor decreases. The excitation capacitance changes for keeping the IM voltage constant by injecting more reactive power into the SEIG. As a general conclusion, the proposed stand-alone power system can withstand step changes in the load and excitation variations and the system has an excellent ability to run smoothly at a wide range of motor loading conditions by changing the excitation levels as a result of changing capacitor bank which indicates the robustness and proves the reliability of the integration between different system components.

References

[1] M. I. Abuashour, T. O. Sweidan, M.S. Widyan, M.M. Hattab and M.A. Ma'itah, "Operational Performance of a PV Generator Feeding DC Shunt and Induction Motors with MPPT", International Journal of Electrical and Computer Engineering (IJECE), Vol. 9, No. 2, pp.771 – 782, April 2019, IAES publishers.

[2] R. C. Bansal, "Three-phase self-excited induction generators: an overview," IEEE Trans. Energy Convers. vol. 20, pp. 292-299, June, 2005.

[3] L. Wang, and J-Y Su, "Dynamic Performance of an Isolated Self-excited Induction Generator under Various Loading Conditions," IEEE Trans. Energy Convers., vol. 14, pp. 93-100, March 1999.

[4] L. Shridhar, B. Singh, C. S. Jha, and B. P. Singh, "Analysis of Self Excited Induction Generator Feeding Induction Motor," IEEE Trans. Energy Convers., vol. 9, pp. 390-396, June 1994.

[5] S. P. Singh, S. K. Jain, and J. Sharma, "Voltage Regulation Optimization of Compensated Self-Excited Induction Generator," IEEE Trans. Energy Convers., vol. 19, pp. 724-732, December 2004.

[6] S. Kuo and L. Wang, "Analysis of Parallel-Operated Self-Excited Induction Generators Feeding an Induction Motor Load with a LongShunt Connection," Electr.Pow. Compo.Sys.,vol 32, pp. 1043-1060, January 2004.

[7] M. Ouali, M. B. A. Kamoun and M. Chaabene, "Investigation on the Excitation Capacitor for a Wind Pumping Plant Using InductionGenerator," Smart Grid and Renewable Energy, vol. 2, pp. 116-125,2011.

[8] T. Sweidan, M. Widyan, and M. Rifai, " Perturbation and Observation as MPPT for Highly Penetrated Grid-Integrated PV Generator Considering Symmetrical Three-Phase Fault ", International Journal of Power and Energy Conversion Vol.10, No.2, 2019.

[9] M.S.Widyan, A.I. Al Tarabsheh, I.Y Etier, R.E Hanitsch,"Dynamic and Steady-State Characteristics of Dc Machines Fed by Photovoltaic Systems", International Journal of Modelling and Simulation, Vol. 30, No. 3, 2010.

[10] M.I. Abuashour, T.O. Sweidan, "Dynamical and Steady State Performance Analysis of DC Series Motor and Induction Motor Powered by an autonomous PV Generator Using MPPT", Int. J. Engineering Systems Modelling and Simulation, Vol. 11, No. 2, pp.68 – 83, 2019.

[11] M.I.Abuashour, T.O. Sweidan, M. S. Widyan, M. M. Hattab and M.A. Ma'itah, "Operational Performance of a PV Generator Feeding DC Shunt and Induction Motors with MPPT", International Journal of Electrical and Computer Engineering (IJECE), Vol. 9, No. 2, pp.771 – 782, April 2019.

[12] T. Sweidan, M. Abuashour, N.Osman, "Transient Analysis of DC Shunt Motor Supplied by Stand-alone PV System Employing FOCV for MPPT ", 2020 Advances in Science and Engineering Technology Multi- Conferences (ASET) , 4-6 Feb 2020, Dubai ,UAE.

[13] T.O.Sweidan, "Dynamical Analysis of DC shunt Motor Powered by PV Generator Using Perturbation and Observation as MPPT Tracking Technique ", Energy and Power Engineering, Vol. 9, pp. 55-69,2017 .

[14] T.O.Sweidan, M.S. Widyan, " Perturbation and Observation as MPPT Algorithm Applied on the Transient Analysis of PV-Powered DC Series Motor", 8th International Renewable Energy Congress (IREC), 21-23 March, 2017.

[15] Kundur, P. (1993) Power System Stability and Control, McGraw Hill, Inc., New York.

[16] Idjdarene K., Rekioua D., Rekioua T., and Tounzi A., "Performance of an isolated induction generator under unbalanced loads," IEEE Trans. on Energy Conversion, vol. 25, pp. 303– 311, 2010.

[17] Dalei J., and Mohanty KB., "A novel method to determine minimum capacitance of the self-excited induction generator", IEEE Tech, pp. 408– 413, 28 February– 2 March , 2014.

[18] Patel, M.R. (1999) Wind and Solar Power System, CRC Press LLC.

[19] Geng, H., Xu, D. and Wuare, B. (2011) 'Direct voltage control for a stand-alone wind-driven self-excited induction generator with improved power quality', IEEE Transaction of Power Electronic, Vol. 26, No. 8, pp.632–641.

[20] A.K. At Jabri and A.I. Alodah, "Capacitance requirements for isolated self-excited induction generator," Proc. IEE, Vol. 137, Part B, No. 3, pp.154-159, May 1990.

[21] Chandratilleke TT., Ho JC. "A study of a photovoltaic array for water pumping," Solar & WindTechnology ,vol. 3, pp.59–71, 1986.

[22] M I. Abuashour, M. Widyan, T. O. Sweidan, M. Momani, "Modeling, Simulations and Operational Performance of a Stand-Alone Hybrid Wind/PV Energy System Supplying Induction Motor for Pumping Applications" Int. J. Engineering Systems Modelling and Simulation, Vol. 10, No. 1, March 2018.

Appendix A

Table A1. Nomenclature

C	Excitation Capacitance
V_{Cd}&V_{Cq}	D&Q axis components of the voltage across the capacitors, respectively
I_{cd}&I_{cq}	D&Q axis components of the capacitors current, respectively
ω_s	Synchronous radian frequency
V_{dsg}	D-axis component of induction generator stator voltage
V_{qsg}	Q-axis component of induction generator stator voltage
V_{drg}	D-axis component of induction generator rotor voltage
V_{qrg}	Q-axis component of induction generator rotor voltage
R_{sg}	Induction generator stator resistance
L_{ssg}	Induction generator stator inductance
L_{mg}	Induction generator mutual inductance between its stator and rotor
ω_{rg}	Induction generator rotor speed
ω_{rm}	Induction motor rotor speed
R_{rg}	Induction generator rotor resistance
L_{rg}	Induction generator rotor inductance
i_{sdg}	D-axis component of induction generator stator current
i_{sqg}	Q-axis component of induction generator stator current
i_{rdrg}	D-axis component of induction generator rotor current
i_{rqg}	Q-axis component of induction generator rotor current
T_{Lg}	Induction generator prime mover torque
J_g	Moment of inertia of induction generator rotor and its prime mover
P_g	Number of poles for induction generator
K_d, K_q	D&Q-axis components of remnant flux at IG rotor, respectively
T_{Lm}	Load torque
V_{dsm}	D-axis component of induction motor stator voltage
V_{qsm}	Q-axis component of induction motor stator voltage
V_{drm}	D-axis component of induction motor rotor voltage
V_{qrm}	Q-axis component of induction motor rotor voltage
R_{sm}	Induction motor stator resistance
L_{ssm}	Induction motor stator inductance
L_{mm}	Induction motor mutual inductance between its stator and rotor windings
R_{rm}	Induction motor rotor resistance
L_{rm}	Induction motor rotor inductance

i_{sdm}	D-axis component of induction motor stator current
i_{sqm}	Q-axis component of induction motor stator current
i_{rdm}	D-axis component of induction motor rotor current
i_{rqm}	Q-axis component of induction motor rotor current
P_m	Number of poles for induction motor
B	Rotor mechanical friction for induction motor
J_m	Moment of inertia of induction motor rotor and the load
V_{ref}	Reference voltage at the controller
V_t	Phase voltage of common coupling bus (CCB)
V_{set}	Voltage difference between reference voltage and phase voltage
T_D&T_M	Controller time constants
IM	Induction motor
IG	Induction generator
SG	Synchronous generator

Appendix B

The following are the technical specifications and numerical values for the constants of the power system.

Wind *turbine*

Number of blades = 3, radius of blade = 4 m, rated wind speed = 9 m/s, gear box ratio = 5.

Self-excited induction generator

7 kW, 127/220V, 40/20A, 60 Hz, 1,800 rpm, four poles, R_{sg} = 0.699 Ω, R_{rg} = 0.799 Ω, L_{ssg} = 42.6mH, J_g = 0.16kg/m2, Kd = 80V, Kq = 80V,

$$Lmg = 0.205im^3 + 0.0053im^2 - 0.0023im + 0.0001$$

Where

$i_m$is the magnetizing current,

$$i_m = \sqrt{(i_{sdg} + i_{rdg})2 + (i_{sqg} + i_{rqg})2}$$

Induction motor

10 kW, 127/220V, 27/15, 60 Hz, 1800 rpm, 4 poles, R_{sm} = 6.5Ω, R_{rm} = 6Ω, L_{mm} = 375μH, L_{sm} = 250mH, L_{rm} = 250mH, J_m = 0.9 kg/m2.